Article:
Bestenlehner, J.M., Vink, J.S., Grafener, G. et al. (2011) The VLT-FLAMES Tarantula Survey III. A very massive star in apparent isolation from the massive cluster R136. Astronomy and Astrophysics, 530. L14. ISSN: 0066-4146

https://doi.org/10.1051/0004-6361/201117043

Astronomy & Astrophysics manuscript no. 17043
May 11, 2011

The VLT-FLAMES Tarantula Survey III: A very massive star in apparent isolation from the massive cluster R136⋆

Joachim M. Bestenlehner[1], Jorick S. Vink[1], G. Gräfener[1], F. Najarro[2], C. J. Evans[3], N. Bastian[4,5], A. Z. Bonanos[6], E. Bressert[5,7,8], P. A. Crowther[9], E. Doran[9], K. Friedrich[10], V. Hénault-Brunet[11], A. Herrero[12,13], A. de Koter[14,15], N. Langer[10], D. J. Lennon[16], J. Maíz Apellániz[17], H. Sana[14], I. Soszynski[18], and W. D. Taylor[11]

(Affiliations can be found after the references)

Received 7 April 2011 / Accepted 2 May 2011

ABSTRACT

VFTS 682 is located in an active star-forming region, at a projected distance of 29 pc from the young massive cluster R136 in the Tarantula Nebula of the Large Magellanic Cloud. It was previously reported as a candidate young stellar object, and more recently spectroscopically revealed as a hydrogen-rich Wolf-Rayet (WN5h) star. Our aim is to obtain the stellar properties, such as its intrinsic luminosity, and to investigate the origin of VFTS 682. To this purpose, we model optical spectra from the VLT-FLAMES Tarantula Survey with the non-LTE stellar atmosphere code CMFGEN, as well as the spectral energy distribution from complementary optical and infrared photometry. We find the extinction properties to be highly peculiar (R_V ∼4.7), and obtain a surprisingly high luminosity $\log(L/L_\odot) = 6.5 \pm 0.2$, corresponding to a present-day mass of $\sim 150 M_\odot$. The high effective temperature of 52.2 ± 2.5kK might be explained by chemically homogeneous evolution – suggested to be the key process in the path towards long gamma-ray bursts. Lightcurves of the object show variability at the 10% level on a timescale of years. Such changes are unprecedented for classical Wolf-Rayet stars, and are more reminiscent of Luminous Blue Variables. Finally, we discuss two possibilities for the origin of VFTS 682: (i) the star either formed *in situ*, which would have profound implications for the formation mechanism of massive stars, or (ii) VFTS 682 is a *slow runaway* star that originated from the dense cluster R136, which would make it the most massive runaway known to date.

Key words. stars: Wolf-Rayet – stars: early-type – stars: atmospheres – stars: mass-loss – stars: fundamental parameters

1. Introduction

Recent claims for the existence of very massive stars (VMS) of up to $300 M_\odot$ at the centre of young clusters like R136 (Crowther et al. 2010) seem to link the formation of such objects to environments in the centres of massive clusters with ∼ 10^4 – 10^5 $M_\odot$. This finding thus appears to support massive star-formation models that invoke competitive accretion and possibly even merging in dense clusters (e.g. Bonnell et al. 2004). Such scenarios emerged after it became clear that the disk-accretion scenario – commonly applied to low- and intermediate star formation – had problems explaining the formation of stars with masses above $10 M_\odot$, as radiation pressure on dust grains would halt and reverse the accretion flow onto the central object (e.g. Yorke & Kruegel 1977). However, recent multi-dimensional hydrodynamical monolithic collapse simulations indicate that massive stars may form via disk accretion after all (e.g. Kuiper et al. 2010). This illustrates that the discussion on clustered vs. isolated massive star formation is still completely open (see de Wit et al. (2005); Parker & Goodwin (2007); Lamb et al. (2010); Bressert et al. in prep.).

In this Letter, we present evidence that VFTS 682 (RA 05h 38m 55.51s DEC -69° 04′ 26.72″) in the Large Magellanic Cloud (LMC), found in isolation from any nearby massive, visible cluster, is one of the most massive stars known. The object suffers from high dust obscuration and is located in, or in the line-of-sight towards, an active star-forming region. On the basis of a mid-infrared (mid-IR) excess, Gruendl & Chu (2009) classified the star as a probable young stellar object (YSO). The VLT-FLAMES Tarantula Survey (VFTS) (Evans et al. 2011) identified it as a new Wolf-Rayet (WR) star,

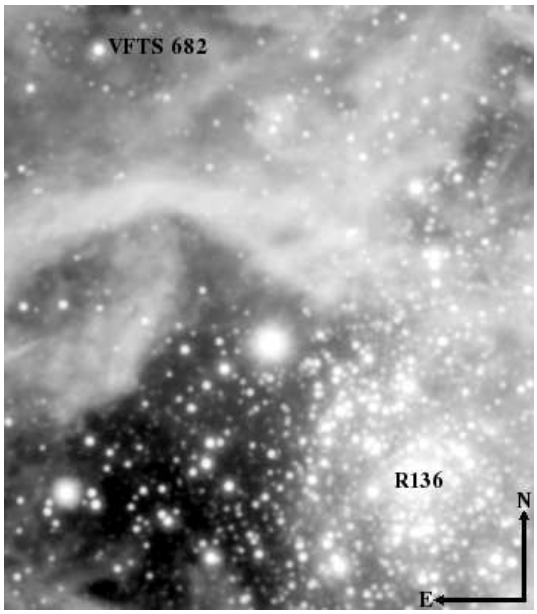

Fig. 1. Combined YJK_s image from the VISTA Magellanic Clouds survey (Cioni et al. 2011). The arrows correspond to 5 pc in the Northern and Eastern directions. The projected distance of VFTS 682 to the cluster R136 is 29 pc (for an assumed LMC distance of 50 kpc).

⋆ Based on observations at the European Southern Observatory Very Large Telescope in programme 182.D-0222.

Table 1. Stellar parameters of VFTS 682

Parameter	Value
$T_\star$	54.5 ± 3 kK
$T_{\rm eff}$	52.2 ± 2.5 kK
$\log(L/L_\odot)$	6.5 ± 0.2
$\log(\dot{M}/\sqrt{f}/M_\odot yr^{-1})$	−4.13 ± 0.2
β	1.6
f	0.25
v_∞	2600 ± 200 km/s
Y[1]	0.45 ± 0.1
$M_{\rm V}$	−6.83 ± 0.12 mag

Notes. (1) Y is the helium mass fraction

at a projected distance approximately 30 pc northeast of R136. Its spectrum was classified as WN5h and is similar to those of the very luminous stars in the core of R136, with strong H, He II, and N IV emission lines. In this Letter, we present a photometric and spectroscopic analysis of VFTS 682 to investigate its origin. The star is relatively faint in the optical, which we argue is the result of significant reddening (with Av ≈ 4.5), implying a high intrinsic luminosity and a mass of order 150 $M_\odot$. The sheer presence of such a massive star outside R136 (and apparently isolated from any notable cluster) poses the question of whether it was ejected from R136 or if it was formed in isolation instead.

2. Spectroscopic Analysis of VFTS 682

The analysis is based on spectroscopic observations (λ4000 – 7000) from MEDUSA mode of VLT-FLAMES (Evans et al. 2011). We first compared observations taken at different epochs (Evans et al. 2011) as to identify potential shifts in the radial velocity (RV) as a result of binarity. To this purpose, we used the N IV λ4060 emission line. With detection probabilities of 96% for a period P<10d, 76% for 10d<P<1yr, and 28% for 1yr<P<5yr, we can basically exclude that VFTS 682 is a short period binary. We found the N V λ4944 line to be particularly useful for RV determinations, as this line remained stable for different wind velocity laws. With particular emphasis on the centroid of the line we obtained 300 ± 10 km/s. If we give more weight to the red wing, we obtain 315 ± 15 km/s, with a similar number for the He II λ4686 line.

For the spectral analysis we use the non-LTE model atmosphere code CMFGEN (Hillier & Miller 1998) which has been developed to provide accurate abundances, stellar parameters, and ionising fluxes for stars dominated by wind emission lines. We use atomic models containing H I, He I-II, C III-IV, N III-V, O III-VI, Si IV, P IV-V, S IV-VI, Fe IV-VII and Ni IV-VI. We made the following assumptions. We adopt a metallicity of half solar with respect to Asplund et al. (2005), and assume N and He to have been enriched by the CNO process. We adopt a 12-fold enhancement of the N mass fraction. We employ a β parameter of 1.6 for the wind velocity law and a wind volume filling factor of $f = 0.25$, assuming that the clumping starts at 10 km/s. In order to estimate the error bars in the stellar temperature ($T_\star$) and mass-loss rate ($\dot{M}$), we computed a grid of models around the preferred values.

The core temperature ($T_\star$) at high optical depth of 54500 ± 3000 K is based on the N IV λ4060 and N V doublet λ4604 and 4620 in emission (Fig. 2). N IV is also sensitive to the mass-loss rate, which is obtained from other lines. The hydrogen and the helium lines are used to determine both the helium abundance (45% by mass) and the mass-loss rate, with $\log(\dot{M}/M_\odot yr^{-1}) = -4.4 \pm 0.2$, where the volume filling factor corrected mass-loss rate is given in Table 1. This value is larger than the $\log(\dot{M}/M_\odot yr^{-1}) = -4.69$ obtained from the mass-loss recipe of Vink et al. (2001) for non-clumped winds. The values can be brought into agreement for a volume filling factor of $f = 0.1$. In the absence of UV spectroscopy of the λ1548, λ1551 C IV doublet, we estimate the terminal velocity (v_∞ = 2600 km/s) from the broadening of the He II and H_α lines. An overview of the stellar parameters and abundances is provided in Table 1.

The stellar parameters of VFTS 682 are similar to those of R136a3 (with a $\log(L/L_\odot) = 6.58$) (Crowther et al. 2010). We note that there are other luminous WNh objects in 30 Dor, for instance, VFTS 617 (=Br 88) which has the same spectral type as VFTS 682 but with weaker emission lines. The spectral analysis of the additional VFTS WNh stars is currently in progress (Bestenlehner et al. in prep.).

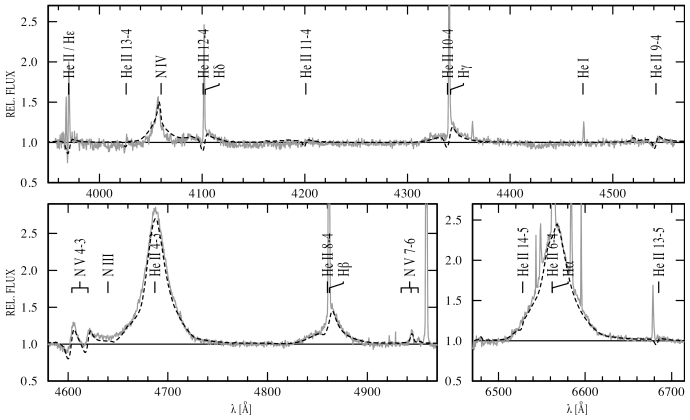

Fig. 2. Relative flux vs. wavelength in Å. Grey solid line: MEDUSA spectrum of VFTS 682. Black dashed line: model spectrum.

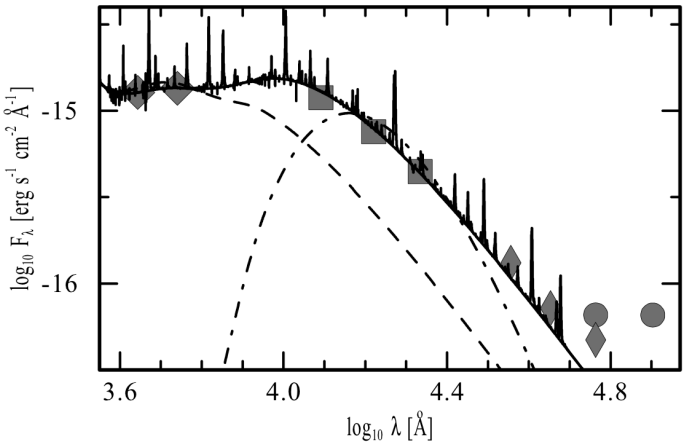

Fig. 3. Log flux vs. log wavelength. Squares: B, V, J, H, K_s photometry, Diamonds: SPITZER SAGE. Circles: SPITZER 5.8 μm and 8.0 μm from Gruendl & Chu (2009). Solid line: SED with anomalous $R_{\rm V}$ parameter. Dashed line: Standard $R_{\rm V}$ parameter. Dashed-Dotted line: attempt to reproduce the NIR excess with a 1500 K black body.

3. Luminosity and Reddening

In its spectral appearance, VFTS 682 is almost identical to that of R136a3 in the core of the dense cluster R136. The luminous

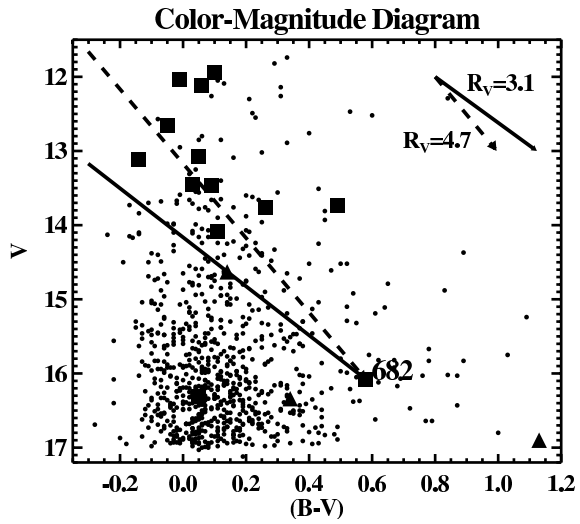

Fig. 4. VFTS objects. Rectangles are WN-stars. Triangles are WC-stars. The arrows in the top right corner are for two different $R_{\rm V}$ values, with a length corresponding to $A_{\rm V} = 1$. The longer lines on the left indicate the transformations between reddened and unreddened CMD positions.

objects in this cluster are thought to be the most massive stars known, with initial masses up to 300 $M_{\odot}$ (Crowther et al. 2010). As VFTS 682 is apparently isolated, and shows no signs of binarity, it offers the opportunity to study such a luminous WN5h object in isolation. The precise luminosity of VFTS 682 is thus of key relevance for this work. Its derivation is however complicated by the large extinction.

Matching the optical photometry with a standard extinction law, i.e., a 'Galactic average' extinction parameter $R_{\rm V} = 3.1$, we obtain a luminosity of $\log(L/L_{\odot}) = 5.7 \pm 0.2$. With this relatively low luminosity we can explain the optical flux distribution, but we fail to match the observed spectral energy distribution (SED) at longer wavelengths. In the near–mid infrared (IR) the observed flux is ~ 3 times higher than the corresponding model flux. Below, we show that we can successfully explain this 'excess' IR emission, including its exact shape, with a reddening parameter $R_{\rm V} = 4.7$, which leads to a much higher stellar luminosity. This effect is visualised in the colour-magnitude diagram (CMD) of Fig. 4. We note that high $R_{\rm V}$ parameters, that deviate from the Galactic average, are not extra-ordinary for massive stars in the LMC (e.g. Bonanos et al. 2011)

3.1. Modelling the near IR flux

Because the extinction in the IR is very low, we can avoid the problems resulting from the uncertain R_V parameter, by choosing the near-IR photometry as our flux standard. In more detail, we derive the luminosity of VFTS 682 by matching B, and V from Parker (1993), and $K_{\rm s}$ from the "InfraRed Survey Facility (IRSF) Magellanic Clouds Point Source Catalog" (Kato et al. 2007) (see Tab. 2). For this purpose we extract the intrinsic B, V, and $K_{\rm s}$ magnitudes from our model, using appropriate filter functions. Based on the resulting values of $E(B-V) = 0.94 \pm 0.02$, and $E(V-K_{\rm s}) = 3.9$, we derive $R_V = A_V/E(B-V)$ for two oft-used extinction laws.

To determine R_V, we use the relations $R_{\rm V} = 1.1994 \times E(V-K_{\rm s})/E(B-V) - 0.183$, as inferred from the extinction law by Cardelli et al. (1989), and $R_{\rm V} = 1.12 \times E(V-K_{\rm s})/E(B-V) + 0.016$, from Fitzpatrick (1999). This way, we obtain $R_{\rm V} = 4.7 \pm 0.1$, $A_{\rm V} = 4.45 \pm 0.12$, and $A_{K_{\rm s}} = 0.55 \pm 0.15$, where the uncertainties refer to the differences in the adopted extinction laws. As A_V is much larger than $A_{K_{\rm s}}$, the derived luminosity mostly relies on $K_{\rm s}$, while the observed values of B, and V mostly determine R_V. Small uncertainties in $B-V$ will thus mainly affect R_V, in a way that the absolute values of B, and V stay the same. As $R_V = A_V/E(B-V)$, this introduces an anti-correlation between the derived R_V, and $E(B-V)$, where A_V is preserved. The resulting luminosity is $\log(L/L_{\odot}) = 6.5 \pm 0.2$, where the error includes uncertainties in the stellar temperature, mass-loss rate, and extinction. The resulting SED fit is presented in Fig. 3.

In an independent analysis of the available UBVIJHK photometry, using the CHORIZOS code (Maíz-Apellániz 2007) for CHi-square cOde for parameteRized modelIng and characteriZation of phOtometry and Spectrophotometry, we obtain $E(B-V) = 0.98 \pm 0.03$, and $R_V = 4.55 \pm 0.17$, which, due to the aforementioned anti-correlation between $E(B-V)$ and R_V, results in an almost unchanged value of $A_V = 4.46 \pm 0.06$. The resulting luminosity, and high R_V are thus confirmed.

Table 2 gives a summary of the available photometry for VFTS 682. In analogy to our previous findings, the differences between the optical photometry of Evans et al. (2011), and Parker (1993) mainly affect $R_{\rm V}$, but not the derived luminosity. Based on the WFI photometry by Evans et al. (2011), we obtain $R_{\rm V} = 5.2 \pm 0.1$ with $E(B-V) = 0.84 \pm 0.02$. The near-IR photometry however has a direct influence on our results. Based on the fainter Two Micron All Sky Survey (2MASS) photometry the derived luminosity decreases by about 0.1dex to $\log(L/L_{\odot}) = 6.4$. In this work, we use the IRSF values, as they connect better to the observed SPITZER MIR photometry.

If we alternatively adopt the standard reddening parameter $R_{\rm V} = 3.1$, and attribute the NIR excess to a second component, such as a cool star and/or a warm (1000-2000 K) dust component (see Fig. 3), we obtain a luminosity of only $\log(L) = 5.7 \pm 0.2$. We note that just one extra component (cool star and/or dust black body) cannot fit the entire SED slope, which implies that we would need a multitude of additional components. These would need to conspire in such a way as to precisely follow our SED. Although we cannot disprove such a configuration, it would be highly contrived.

To summarise, the most likely luminosity of VFTS 682 is $\log(L) = 6.5 \pm 0.2$, which would support the high luminosities that have been derived by Crowther et al. (2010) for the VMS in the core of R 136.

3.2. The MIR excess

We also investigate the issue of whether VFTS 682 has a mid-IR excess in SPITZER data. We compared two sources of MIR photometry, the "Surveying the Agents of a Galaxy's Evolution (SAGE) IRAC Catalog" for point sources (Meixner et al. 2006) as well as the recent YSO catalog of Gruendl & Chu (2009). In contrast to the SAGE IRAC Catalog, Gruendl & Chu (2009) included spatially more extended sources. The MIR photometry data from both sources are listed in Table 2. Gruendl & Chu (2009) detected a mid-IR excess at 5.8 and 8.0 μm and categorised VFTS 682 as a YSO candidate. We are not able to confirm the MIR excess on the basis of the SAGE IRAC Catalog photometry, but the difference in the two data sources may be explained in the following way.

The MIR point-source data of Meixner et al. (2006) basically follow the slope of our optical-to-NIR fit continued into the MIR, whilst the larger scale MIR data of Gruendl & Chu (2009) show a

Table 2. Apparent Magnitude of VFTS 682

	U	B	V	I
Evans et al. (2011)	–	16.66	16.08	
Parker (1993)	16.40	16.75	16.11	
DENIS (2005)				14.89
	J	H	K_s	
IRSF[1]	13.55	12.94	12.46	
2MASS	13.73	13.08	12.66	
	$3.6\mu m$	$4.5\mu m$	$5.8\mu m$	$8.0\mu m$
SAGE	11.73	11.42	10.84	–
Gruendl & Chu (2009)	11.69	11.37	10.48	9.15

Notes. [(1)] Transformed to the 2MASS system.

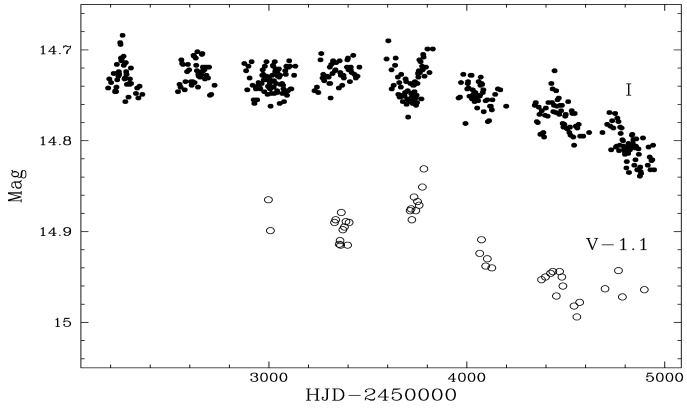

Fig. 5. OGLE III V and I lightcurves for VFTS 682 during 2001-2009.

clear MIR excess. Whereas the MIR excess could be consistent with an extended circumstellar shell, such as recently detected in SPITZER 24 micron images of the Galactic Centre WNh star WR102ka (Barniske et al. 2008), there is no evidence for such a shell (or bowshock) in SPITZER 8 micron images of VFTS 682 at similar angular scales as for WR102ka. However, given the resolution limit of ∼ 2 arcsec the IR excess might be due to an unresolved circumstellar shell with a diameter of < 0.5 pc.

4. Variability on timescales of years

To study the stability of VFTS 682 we show Optical Gravitational Lensing Experiment (OGLE-III) lightcurves (Udalski et al. 2008) in V and I in Fig. 5. On top of the short-term jitter, the object clearly dimmed by ∼0.1 mag in both the V and I band during the years 2006-2009. Furthermore, the object shows an increase in the K-band by ∼0.15 mag during 2010 (Evans et al. in prep.). This kind of long-term variability is unprecedented for Wolf-Rayet stars, and is more characteristic for Luminous Blue Variables (LBVs). However, we note that the nature of these changes is not the same as those of bona-fide LBVs with S Doradus cycles of 1-2 mag variations (Humphreys & Davidson 1994).

5. Discussion on the origin of VFTS 682

VFTS 682 is located in an active star-formation region of 30 Dor (Johansson et al. 1998). It is not anywhere close to the core of R136, or – as far as we can tell – to any other nearby cluster. This might be considered a surprise as VMS are normally found in the cores of large clusters, such as the Arches cluster or R136. By contrast, VFTS 682 is rather isolated at a projected distance of 29 pc from R136. This raises the question of whether the object formed *in situ* or is a *slow* runaway object from R136 instead.

In order to address these issues, we provide some velocity estimates. The measured RV shift of VFTS 682 is $v_r \approx 300$ km/s, which is somewaht higher than the average velocity in 30 Dor (∼ 270±10 km/s, Sana et al. in prep, Bosch et al. 2009). If VFTS 682 is a runaway from R136, it would require a tangential velocity of 30 km/s to appear at a projected distance of 30 pc within approximately 1 Myr. Together with an RV offset of ∼30 km/s, VFTS 682 would then require a true velocity of ∼40 km/s, i.e. at the lower range of velocities for classical OB runaway stars (e.g. Philp et al. 1996). Still, this would make it the most massive runaway star known to date.

In case the object is a runaway star, a bow shock might potentially be visible as VFTS 682 is surrounded by dust clouds. Whilst there is currently no evidence for a bow shock, one of the possible explanations for the MIR excess is the presence of a bow-shock (e.g. Gvaramadze et al. 2010). Alternative explanations for the MIR excess may involve its (line-of-sight) association with an active star forming region, or a nebula formed by vigorous mass loss since the object started to burn hydrogen in its core. In this context, it may or may not be relevant that VFTS 682 shows slow photometric variations suggestive of LBVs that may suffer from mass ejections.

The most probable luminosity of VFTS 682 is $\log(L) = 6.5 \pm 0.2$. The question is what stellar mass the object corresponds to, and what is its most likely evolutionary age. The high temperature places the object right on the zero-age main sequence (ZAMS), which can be best understood as a result of chemically homogeneous evolution (CHE). Such an evolution has also been proposed for two WR stars in the SMC (Martins et al. 2009). Note that this type of evolution has been suggested for the production of long gamma-ray bursts (Yoon & Langer 2005). In order to obtain a meaningful mass limit, we employ the recent mass-luminosity relationships by Gräfener et al. (2011) for homogeneous hydrogen burners. Utilising the derived He abundance (Y=0.45), the most likely present-day mass is $\sim 150 M_{\odot}$. In detailed stellar evolution models of Brott et al. (2011) and Friedrich et al. (in prep), CHE is achieved through rapid rotation, with $v_{\rm rot}^{\rm init} > 200$km/s. A value of Y=0.45 is obtained at an age of 1-1.4 Myrs and the initial mass would be of $\sim 120 - 210 M_{\odot}$, where the mass range is defined through the uncertainty in the luminosity.

Finally, from our analysis it is clear that VFTS 682 is a very massive object. It is often assumed that such massive objects can only be formed in dense cluster environments, where they are normally found. The apparent isolation of VFTS 682 may thus represent an interesting challenge for dynamical ejection scenarios and/or massive star formation theory.

References

Asplund, M., Grevesse, N., & Sauval, A. J. 2005, ASPCS, 336, 25
Barniske, A., Oskinova, L. M., & Hamann, W. 2008, A&A, 486, 971
Bonanos, A. Z., Castro, N., Macri, L. M., & Kudritzki, R. 2011, ApJ, 729, L9+
Bonnell, I. A., Vine, S. G., & Bate, M. R. 2004, MNRAS, 349, 735
Bosch, G., Terlevich, E., & Terlevich, R. 2009, AJ, 137, 3437
Brott, I., de Mink, S. E., Cantiello, M., et al. 2011, ArXiv:1102.0530
Cardelli, J. A., Clayton, G. C., & Mathis, J. S. 1989, ApJ, 345, 245
Cioni, M., Clementini, G., Girardi, L., et al. 2011, A&A, 527, A116+
Crowther, P. A., Schnurr, O., Hirschi, R., et al. 2010, MNRAS, 408, 731
de Wit, W. J., Testi, L., Palla, F., & Zinnecker, H. 2005, A&A, 437, 247
DENIS. 2005, VizieR Online Data Catalog, 1, 2002
Evans, C. J., Taylor, W. D., Henault-Brunet, V., et al. 2011, ArXiv:1103.5386

Fitzpatrick, E. L. 1999, PASP, 111, 63
Gräfener, G., Vink, J. S., de Koter, A., & Langer, N. 2011, A&A submitted
Gruendl, R. A. & Chu, Y. 2009, ApJS, 184, 172
Gvaramadze, V. V., Kroupa, P., & Pflamm-Altenburg, J. 2010, A&A, 519, A33+
Hillier, D. J. & Miller, D. L. 1998, ApJ, 496, 407
Humphreys, R. M. & Davidson, K. 1994, PASP, 106, 1025
Johansson, L. E. B., Greve, A., Booth, R. S., et al. 1998, A&A, 331, 857
Kato, D., Nagashima, C., Nagayama, T., et al. 2007, PASJ, 59, 615
Kuiper, R., Klahr, H., Beuther, H., & Henning, T. 2010, ApJ, 722, 1556
Lamb, J. B., Oey, M. S., Werk, J. K., & Ingleby, L. D. 2010, ApJ, 725, 1886
Maíz-Apellániz, J. 2007, ASPCS, 364, 227
Martins, F., Hillier, D. J., Bouret, J. C., et al. 2009, A&A, 495, 257
Meixner, M., Gordon, K. D., Indebetouw, R., et al. 2006, AJ, 132, 2268
Parker, J. W. 1993, AJ, 106, 560
Parker, R. J. & Goodwin, S. P. 2007, MNRAS, 380, 1271
Philp, C. J., Evans, C. R., Leonard, P. J. T., & Frail, D. A. 1996, AJ, 111, 1220
Udalski, A., Szymanski, M. K., Soszynski, I., et al. 2008, Acta Astron., 58, 69
Vink, J. S., de Koter, A., & Lamers, H. J. G. L. M. 2001, A&A, 369, 574
Yoon, S. & Langer, N. 2005, A&A, 443, 643
Yorke, H. W. & Kruegel, E. 1977, A&A, 54, 183

---

[1] Armagh Observatory, College Hill, Armagh BT61 9DG, United Kingdom
[2] Centro de Astrobiología (CSIC-INTA), Ctra. de Torrejón a Ajalvir km-4, E-28850 Torrejón de Ardoz, Madrid, Spain
[3] UK Astronomy Technology Centre, Royal Observatory Edinburgh, Blackford Hill, Edinburgh, EH9 3HJ, UK
[4] Excellence Cluster Universe, Boltzmannstr. 2, 85748 Garching, Germany
[5] School of Physics, University of Exeter, Stocker Road, Exeter EX4 4QL, UK
[6] Institute of Astronomy & Astrophysics, National Observatory of Athens, I. Metaxa & Vas. Pavlou Street, P. Penteli 15236, Greece
[7] European Southern Observatory, Karl-Schwarzschild-Strasse 2, D87548, Garching bei München, Germany
[8] Harvard-Smithsonian CfA, 60 Garden Street, Cambridge, MA 02138, USA
[9] Dept. of Physics & Astronomy, Hounsfield Road, University of Sheffield, S3 7RH, UK
[10] Argelander-Institut für Astronomie der Universität Bonn, Auf dem Hügel 71, 53121 Bonn, Germany
[11] SUPA, IfA, University of Edinburgh, Royal Observatory Edinburgh, Blackford Hill, Edinburgh, EH9 3HJ, UK
[12] Departamento de Astrofísica, Universidad de La Laguna, E-38205 La Laguna, Tenerife, Spain
[13] European Southern Observatory, Alonso de Cordova 1307, Casilla, 19001, Santiago 19, Chile
[14] Astronomical Institute Anton Pannekoek, University of Amsterdam, Kruislaan 403, 1098 SJ, Amsterdam, The Netherlands
[15] Astronomical Institute, Utrecht University, Princetonplein 5, 3584CC, Utrecht, The Netherlands
[16] ESA, Space Telescope Science Institute, 3700 San Martin Drive, Baltimore, MD 21218, USA
[17] Instituto de Astrofísica de Andalucía-CSIC, Glorieta de la Astronomía s/n, E-18008 Granada, Spain
[18] Warsaw University Observatory, Aleje Ujazdowskie 4, 00-478 Warsaw, Poland